

PHYSICAL CHEMISTRY  
OF NANOCCLUSERS AND NANOMATERIALS

## Effect of the Titanium Dioxide Shell on the Plasmon Properties of Silver Nanoparticles

D. A. Afanasyev, N. Kh. Ibrayev, T. M. Serikov, and A. K. Zeinidenov

*Institute of Molecular Nanophotonics, Buketov Karaganda State University, Karaganda, Kazakhstan*

*e-mail: niazibrayev@mail.ru, a\_d\_afanasyev@mail.ru*

Received April 22, 2015

**Abstract**—The results of the synthesis of Ag–TiO<sub>2</sub> nanostructures were presented. The optical properties of silver nanoparticles and Ag–TiO<sub>2</sub> structures were studied. The size and shape of Ag–TiO<sub>2</sub> nanostructures were determined. The electron density in silver, the damping constant of plasma oscillations, and the ratio between the masses of the Ag core and the TiO<sub>2</sub> shell were determined from the absorption spectra of Ag and Ag–TiO<sub>2</sub> solutions. It was shown that the semiconductor shell of titanium dioxide leads to a decrease in the electron density in silver nanoparticles and the damping constant of plasma oscillations.

**Keywords:** titanium dioxide, plasmon resonance, silver nanoparticle.

**DOI:** 10.1134/S0036024416040026

### INTRODUCTION

In recent years, interest in nanomaterials based on titanium dioxide has been steadily growing in view of their unique physicochemical properties. This is dictated by the wide use of TiO<sub>2</sub> for solving various problems. Thus, nanomaterials based on titanium dioxide are used for photocatalysis [1, 2], solar power engineering [3, 4], water and air purification from organic pollutants, and elimination of bacteria [5]. As is known, TiO<sub>2</sub> is well compatible with human tissues and can be used in medicine [6].

The electronic and energy-band structure of crystalline TiO<sub>2</sub> was studied in detail in [7–9]. Titanium dioxide has a wide band gap, and its photocatalytic properties start to show themselves in the UV region of the spectrum. This is often a limiting factor for its applications. Therefore, it is important to perform studies aimed at enhancing the photostimulated electronic processes in the functional materials based on titanium dioxide. The spectral sensitivity can be expanded to the visible range by doping TiO<sub>2</sub> with various impurities [10, 11]. One of the methods to enhance the photocatalytic and photovoltaic properties of nanomaterials based on titanium dioxide is to use localized surface plasmon resonance (LSPR) of metal nanoparticles (NPs) [12, 13].

An interesting solution is the creation of nanosystems with an (Ag) core–(TiO<sub>2</sub>) shell structure. This geometrical construction can be used in dye-sensitized solar cells [13, 14]. The semiconductor shell is expected to protect the metal NPs from oxidation, and

the plasmon core will increase light absorption by dye molecules sorbed on the TiO<sub>2</sub> surface.

This paper reports on the results of our studies of the optical properties of the colloid solutions of silver NPs and Ag–TiO<sub>2</sub> structures. A number of important optical and electrophysical parameters and the ratio between the masses of Ag and TiO<sub>2</sub> can be determined from the absorption spectra of Ag–TiO<sub>2</sub> solutions.

### EXPERIMENTAL

A colloid solution of silver NPs was synthesized by chemical reduction of metal ions from the silver nitrate (AgNO<sub>3</sub>) in an ethanol solution. Sodium borohydride (NaBH<sub>4</sub>) was used as a reducing agent. This choice of reducer was dictated by the high reducing ability of sodium borohydride, which is simultaneously a reducer and stabilizer for silver NPs [15, 16]. The procedure for obtaining silver NPs was as follows. Sodium borohydride (0.001 g) was dissolved in ethanol (25 mL). A solution of silver nitrate (0.0045 g per 10 mL of solvent) was dissolved in ethanol. A solution of sodium borohydride cooled to –2°C was added in several 50 μL portions, while constantly stirring, to the resulting AgNO<sub>3</sub> solution. The color of the solution changed from transparent to dark brown, which indicated the formation of silver NPs.

The TiO<sub>2</sub> semiconductor shell was obtained by the procedure of [13]. Freshly prepared ethanol solutions of silver NPs and titanium tetraisopropoxide (TTIP) were used. The TiO<sub>2</sub> shell was synthesized by mixing the ethanol solutions of TTIP and silver NPs while thoroughly stirring the mixtures. The resulting mix-

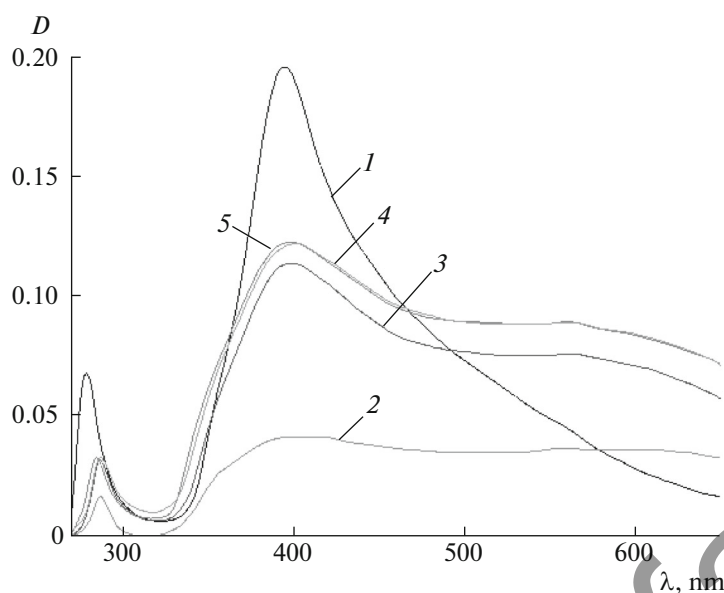


**Fig. 1.** Absorption spectra of silver nanoparticles in ethanol solution: (1) after the synthesis; (2) in 24 h after the synthesis; (3), (4), and (5) after treatment in an ultrasonic bath for 10, 20, and 30 min, respectively.

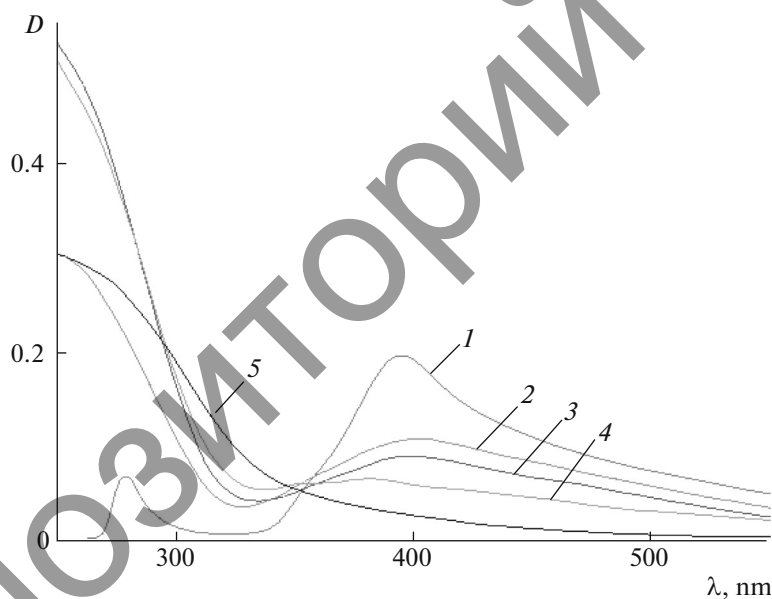


**Fig. 2.** Absorption spectra of silver NPs in ethanol at TTIP concentrations of (1) 0, (2) 0.002, (3) 0.01, and (4) 0.05 M; (5) absorption spectrum of the ethanol solution of TTIP with a concentration of 0.002 M.

ture was stirred for 12 h on a PTR-35 multifunctional rotator at room temperature in the dark.

The absorption spectra of the synthesized colloid solutions were recorded with a Solar CM2203 spectrophotometer. The size of the resulting structures was measured using a Zetasizer Nano ZS (Malvern Instruments, Great Britain) submicron particle size analyzer. The shape of nanoparticles was determined with a TESCAN Mira 3 scanning electron microscope.

## RESULTS AND DISCUSSION

The absorption spectrum of silver NPs in an ethanol solution is shown in Fig. 1 (curve 1). The presence of an absorption band with a maximum at 394 nm and with a half-width of  $\Delta\lambda_{1/2}^{\text{abs}} = 95$  nm points to the formation of silver NPs. The absorption spectrum also contains a short-wave absorption band, which was also reported in [17, 18]. The absorption spectrum of the same solution was measured in 24 h to determine the

**Table 1.** Amount of TiO<sub>2</sub> in the Ag/TiO<sub>2</sub> system (*m*, %) depending on the TTIP concentration (*c*, M)

<i>c</i>	<i>m</i>
0.002	25
0.01	40
0.05	45

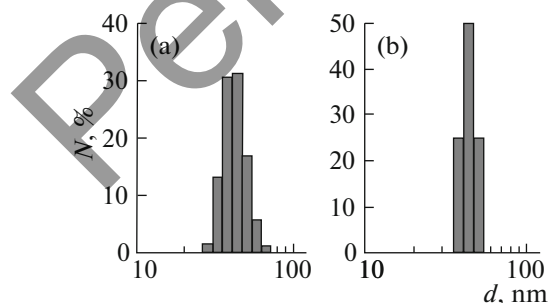
**Table 2.** Main characteristics of Ag and Ag/TiO<sub>2</sub> nanoparticles (*c* is the TTIP concentration in solution)

NP material	$N \times 10^{-22}, \text{cm}^{-3}$	$\gamma \times 10^{-15}, \text{s}^{-1}$
Ag	8.25	1.98
Ag/TiO <sub>2</sub> ( <i>c</i> = 0.002 M)	7.93	1.90
Ag/TiO <sub>2</sub> ( <i>c</i> = 0.01 M)	7.93	1.90

stability of silver NPs in an ethanol solution. In this case, the optical density decreased and the spectrum shape changed because of the appearance of an additional maximum in the range 560–580 nm (curve 2, Fig. 1). The observed changes in the absorption spectrum are evidently caused by aggregation of silver NPs [19, 20]. When the silver colloid solution was treated in an ultrasonic bath for 10–30 min, the aggregates dispersed, as indicated by the partial increase in the optical density in the absorption band of silver NPs (curves 3–5, Fig. 1). A complete dispersion of aggregates was not achieved, and they showed themselves as a wide absorption band with a maximum in the range 560–580 nm.

To synthesize the titanium dioxide semiconductor shell, we used freshly prepared colloid solutions of silver NPs. To prepare the Ag–TiO<sub>2</sub> structures with different shell thicknesses, the TTIP concentration in the solution was varied. TTIP at concentrations of 0.002–0.05 M was added in a reaction vessel containing 1 mL of the prepared solution of silver NPs.

Figure 2 shows the absorption spectra of the ethanol solution of Ag NPs with TTIP additions. The optical density in the absorption band of Ag NPs decreases

**Fig. 3.** Size distribution of (a) silver NPs and (b) Ag NPs–TiO<sub>2</sub> after the addition of 0.05 M TTIP.

as the TTIP concentration increases, and the maximum of the absorption band experiences a small long-wave shift (curves 2 and 3).

According to the data of optical density measurements in the UV range in which titanium dioxide absorbs [21, 22], the absorption intensity increases with the TTIP concentration in solution, which points to the formation of TiO<sub>2</sub> (curves 2–4, Fig. 2). A comparison of the absorption spectrum of the binary solution with 0.002 M TTIP (curve 2) with the spectrum of the pure ethanol solution of TTIP with the same concentration (curve 5) showed that the spectra did not fully coincide, despite the coincidence of optical densities at 250 nm.

A comparison of curves 2–4 (Fig. 2) with curves 2–5 (Fig. 1) shows that addition of TTIP to the solution of silver NPs did not lead to aggregation of Ag NPs. This is indicated by the absence of a long-wave maximum characteristic of silver NP aggregates. For the solutions whose spectra are shown Fig. 2, the size of the synthesized Ag, TiO<sub>2</sub>, and Ag–TiO<sub>2</sub> particles was measured by dynamic laser light scattering [23]. The size measurements of colloid Ag particles showed that the solution contained NPs with a mean size of ~34 nm (Fig. 3a). At the same time, the solution had a small (up to 0.1%) amount of large particles with a mean size of ~160 nm, which should be attributed to silver NP aggregates. After the synthesis of the semiconductor shell, the measurements showed that the solution contained particles with a size of ~44 nm at a TTIP concentration of 0.05 M (Fig. 3b). Particles with different sizes were not detected. For the ethanol solution of TTIP with a concentration of 0.002 M, the measurements revealed the formation of particles with a size of 200 nm and an increase in the particle size to 246 nm in 12 h after the synthesis.

Thus, the appearance of nanoparticles with a size of ~44 nm after the addition of TTIP in the solution of Ag NPs and the absence of nanoparticles with other sizes in the solution suggests the formation of a semiconductor shell of titanium dioxide, but not the formation of TiO<sub>2</sub> nanoparticles separately from silver NPs.

The electron microscopy studies revealed the formation of spherical Ag–TiO<sub>2</sub> structures (Fig. 4).

For nanosized metal particles, the position of the plasmon absorption band can be described by the following equations [12]:

$$\lambda_{\text{peak}}^2 = \lambda_p^2 (\epsilon^\infty + 2\epsilon_m), \quad (1)$$

$$\lambda_p^2 = 4\pi^2 c^2 m \epsilon_0 / Ne^2, \quad (2)$$

where  $\lambda_p^2$  is the volume plasma wavelength in terms of the electron mass,  $\epsilon_0$  is the vacuum dielectric constant,  $e$  is the electron charge,  $N$  is the electron density,  $\epsilon^\infty$  is the high-frequency dielectric permittivity of silver ( $\sim 4.9 \pm 0.3$ ), and  $\epsilon_m$  is the numerical value equivalent

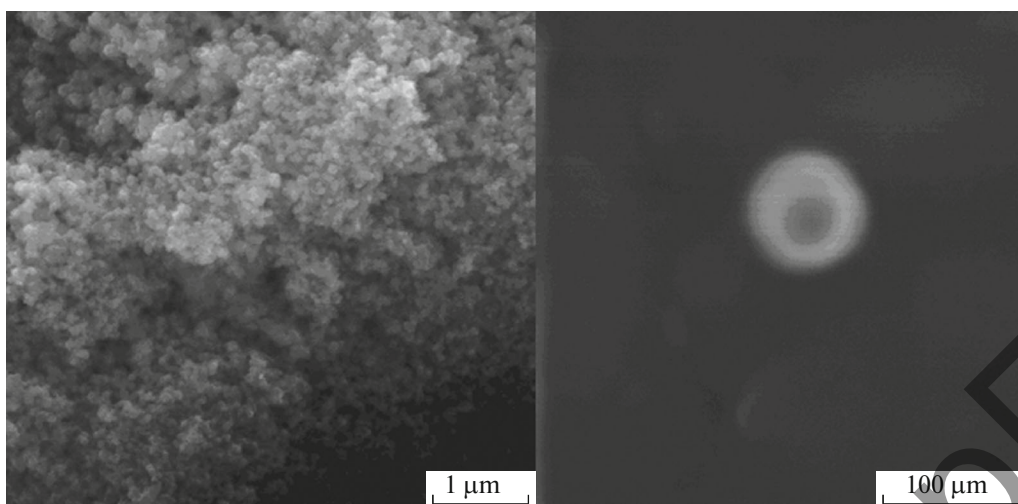


Fig. 4. Electron microscopy image of Ag–TiO<sub>2</sub> structures.

to the square of solvent refraction; for ethanol,  $\varepsilon_m = 1.85$  was determined from the refraction index  $n_m$  [24].

When a titanium dioxide shell forms on the surface of silver NPs, the electron density of silver  $N$  is expected to decrease [25]. This, in turn, will lead to an increase in  $\lambda_p^2$  (Eq. (2)) corresponding to a long-wave shift of the plasmon resonance (PR) maximum. The decrease in the electron density  $N$  will also lead to a decrease in the absorption intensity of PR, which was just observed in the experiment (Fig. 2). These results indicate that the formation of a TiO<sub>2</sub> film occurs on the surface of Ag NPs. At the same time, the effect of the change in the dielectric permittivity of the medium ( $\varepsilon$ ) around the Ag core on the long-wave shift of the

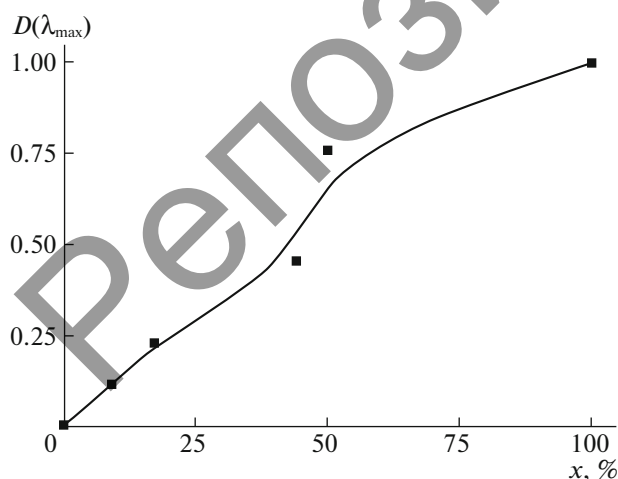


Fig. 5. Ratio between the relative optical density ( $D$ ) of the solution of Ag NPs–TiO<sub>2</sub> and the mass fraction of silver in Ag NPs–TiO<sub>2</sub> ( $x$ ).

absorption maximum of silver nanoparticles should not be excluded [16, 26].

A plot of the mass ratio between the Ag core and the semiconductor TiO<sub>2</sub> shell was constructed using the experimental data of [27, 28] (Fig. 5). The mass ratios for Ag–TiO<sub>2</sub> structures, whose spectral data are shown in Fig. 3, were determined from the obtained dependence. The results of calculations are given in Table 1.

According to [29, 30], if the radius of plasmon metal NPs is smaller than the incident wavelength, the following linear dependence is applicable:

$$\frac{1}{k} = \frac{\theta_2}{\theta_1} + \frac{1}{\theta_1} \left( \frac{\lambda_{\text{peak}}^2}{\lambda} - \lambda \right)^2. \quad (3)$$

The parameters of the plasmon effect can be determined from the plot of the dependence of  $\frac{1}{k}$  on

$\left( \frac{\lambda_{\text{peak}}^2}{\lambda} - \lambda \right)^2$ . Figure 6 shows the dependence of  $\frac{1}{k}$  on

$\left( \frac{\lambda_{\text{peak}}^2}{\lambda} - \lambda \right)^2$  for the colloid silver solution. The  $\theta_1$  and

$\theta_2$  parameters were determined from the linear part of the plot. Using these parameters, we can determine the damping constant of plasma oscillations  $\gamma$ .

$$\gamma = \frac{2\pi c \theta_2^{1/2}}{\lambda_{\text{peak}}^2}. \quad (4)$$

The calculated electron densities  $N$  (Eqs. (1) and (2)) and the damping constant of plasma oscillations  $\gamma$  (Eq. (4)) are listed in Table 2. According to Table 2, the  $N$  and  $\gamma$  values correlate with each other; when the TiO<sub>2</sub> semiconductor shell forms, the concentration of electrons in silver decreases.

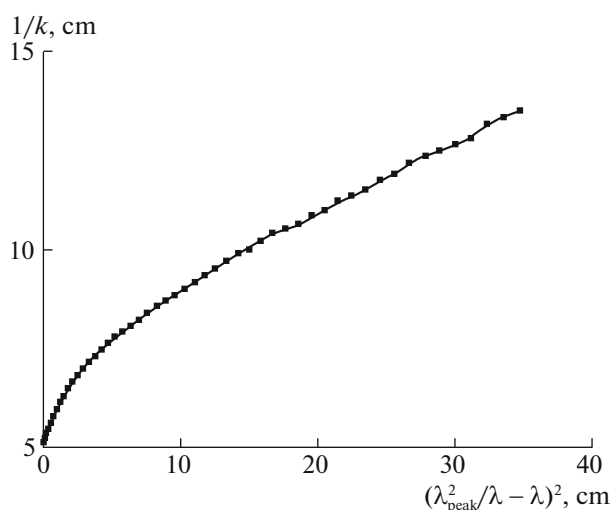


Fig. 6. Dependence of  $1/k$  on  $\lambda$  for the colloid solution of silver.

Thus, the optimum conditions for the synthesis of Ag–TiO<sub>2</sub> nanostructures were determined. The spectral data of the solutions show that an increase in the titanium tetraisopropoxide concentration leads to an increase in the thickness of the synthesized TiO<sub>2</sub> shell. The ratio between the masses of the Ag core and the TiO<sub>2</sub> shell was determined from the absorption spectra of Ag–TiO<sub>2</sub> solutions. In the presence of a semiconductor shell, the electron density in silver NPs and the damping constant of plasma oscillations were found to decrease.

## REFERENCES

1. A.-M. A. Abdel-Wahab and A. E.-A. M. Gaber, *J. Photochem. Photobiol. A* **114**, 213 (1998).
2. *Photocatalytic Purification of Water and Air*, Ed. by D. F. Ollis and H. Al-Ekabi (Elsevier, Amsterdam, 1993).
3. B. O'Regan and M. Gratzel, *Nature* **353**, 737 (1991).
4. S. Ito, T. N. Murakami, P. Comte, et al., *Thin Solid Films* **516**, 4613 (2008).
5. Ch. Goebbert, in *Handbook for Cleaning/Decontamination of Surfaces*, Ed. by I. Johansson and P. Somasundaran (Elsevier, Amsterdam, 2007).
6. V. Zinoviev, A. Eydokimov, E. Belanov, et al., *Antiviral Res.* **78**, A51 (2008).
7. G. P. Luchinskii, *The Chemistry of Titanium* (Khimiya, Moscow, 1971) [in Russian].
8. S. Mo and W. Ching, *Phys. Rev. B* **51**, 13023 (1995).
9. M. Landmann, E. Rauls, and W. G. Schmidt, *J. Phys.: Condens. Matter* **24**, 195503 (2012).
10. Yu. V. Pleskov, *Solar Energy Conversion: A Photoelectrochemical Approach* (Khimiya, Moscow, 1990) [in Russian].
11. Sh. M. Gupta and M. J. Tripathi, *Chin. Sci. Bull.* **56**, 1639 (2011).
12. P. Calandra, A. Ruggirello, A. Pistone, and V. T. Liveri, *J. Clust. Sci.* **21**, 767 (2010).
13. J. Qi, X. Dang, P. T. Hammond, and A. M. Belcher, *ACS Nano*, No. **5**, 7108 (2011).
14. K. Guo, M. Li, X. Fang, et al., *J. Power Sources* **230**, 55 (2013).
15. I. Dragieva, G. Ivanova, S. Bliznakov, et al., *Phys. Chem. Glass.* **41**, 264 (2000).
16. M. U. Rashid, M. K. H. Bhuiyan, and M. E. Quayum, *Dhaka Univ. J. Pharm. Sci.* **12**, 29 (2013).
17. U. Kreibitz, *Z. Phys.* **234**, 307 (1970).
18. S. Silvestrini, T. Carofiglio, and M. Maggini, *Chem. Commun.* **49**, 84 (2013).
19. R. Gill, L. Tianb, H. Amerongen, and V. Subramaniam, *Phys. Chem. Chem. Phys.* **15**, 15734 (2013).
20. M. Mancuso, L. Jiang, E. Cesarman, and D. Erickson, *Nanoscale* **5**, 1678 (2013).
21. N. Serpone, D. Lawless, and R. Khairutdinov, *J. Phys. Chem.* **99**, 16646 (1995).
22. N. Ghrairi and M. Bouaicha, *Nanoscale Res. Lett.* **7**, 357 (2012).
23. B. J. Berne and R. Pecora, *Dynamic Light Scattering. With Applications to Chemistry, Biology, and Physics* (General Publ. Company, Toronto, 2000).
24. V. A. Rabinovich and Z. Ya. Khavin, *Concise Handbook of Chemistry* (Khimiya, Leningrad, 1978) [in Russian].
25. W. Wang, J. Zhang, F. Chen, et al., *J. Colloid Interface Sci.* **323**, 182 (2008).
26. S. Angkaewa and P. Limsuwana, *Proc. Eng.* **32**, 649 (2012).
27. P. Wang, D. Wang, T. Xie, et al., *Mater. Chem. Phys.* **109**, 181 (2008).
28. X. Yin, W. Que, Y. Liao, et al., *Colloids Surf. A: Physicochem. Eng. Asp.* **410**, 153 (2012).
29. A. V. Toporko, V. V. Tsvetkov, V. D. Yagodovskii, and A. Issa, *Zh. Fiz. Khim.* **69**, 867 (1995).
30. L. N. Podlegaeva, D. M. Rusakov, S. A. Sozinov, et al., *Vestn. Kemer. Univ.*, No. **2**, 91 (2009).

Translated by L. Smolina